

Received November 25, 2020, accepted December 3, 2020, date of publication December 14, 2020, date of current version December 29, 2020.

Digital Object Identifier 10.1109/ACCESS.2020.3044346

Low Gain Ripple and DC-Grounded Slant-Polarized Formulation With 360° Broadbeam Coverage

MUHAMMAD SHAHZAD SADIQ¹, (Graduate Student Member, IEEE),
CUNJUN RUAN^{1,2}, (Senior Member, IEEE), HAMZA NAWAZ³, SHAHID ULLAH¹,
AND WENLONG HE⁴, (Member, IEEE)

¹School of Electronic and Information Engineering, Beihang University, Beijing 100191, China

²Beijing Key Laboratory for Microwave Sensing and Security Applications, Beihang University, Beijing 100191, China

³Department of Electronics Engineering, Shanghai Jiao Tong University, Shanghai 200240, China

⁴College of Electronics and Information Engineering, Shenzhen University, Shenzhen 518060, China

Corresponding author: Cunjun Ruan (ruancunjun@buaa.edu.cn)

This work was supported in part by the National Natural Science Foundation of China under Grant 61831001, in part by the High-Level Talent Introduction Project of Beihang University under Grant ZG216S1878, and in part by the Youth-Top-Talent Support Project of Beihang University under Grant KG12060401.

ABSTRACT In this paper, a new slant-polarized slot antenna configuration is presented for direction finding and base station applications. The proposed antenna comprises enhanced size coaxial cables, slots, and feeding assemblies. The slant polarization is achieved by four angled slots etched around the outer cylinder of the oversized coaxial cable. An internal compact axis-symmetric feeding network connects primary apertures to form the omnidirectional antenna. Simulations and measurements demonstrate that the antenna maintains an omnidirectional pattern from 2.5 GHz to 2.8 GHz, having 11.3% bandwidth (measured return loss < -10 dB) and gain ripple of ± 0.2 dB in the azimuth plane, which leads to the stable operational coverage. Another benefit of this structure is its polarization purity. The cross-polarization levels are below -14dB over the whole bandwidth. Move over, it is ruggedized DC short, self-supporting, and surface-mountable structure. Furthermore, compact and conformal shape reduces aerodynamic drag and makes this antenna a potential candidate for mounting vehicle systems too.

INDEX TERMS Omnidirectional, gain ripple, slant polarization, dc ground, rugged.

I. INTRODUCTION

Antennas are always considered to be an essential part of communication systems [1]–[3].

Spectrum sensing and Direction Finding (DF) systems are widely used for locating and suppressing unwanted communications in war or search and rescue operations in peacetime. Such systems usually incorporate omnidirectional antennas because of the ease of phase calculation of the incoming signal [4], [5]. Their azimuth radiation pattern or 360 omnidirectional patterns should be free to gain ripples because these ripples lead to error in calculating range and the angle of the target [6]. Cellular communication (LTE) implements the Small cell or ultra-small cell equipment

The associate editor coordinating the review of this manuscript and approving it for publication was Yang Yang¹.

having omnidirectional antennas so that the coverage area is tessellated smoothly even in shadowed region [7]; Such applications require a rugged antenna having an omnidirectional pattern with reduced azimuthal gain variations within a compact size.

In the above applications, there are always two scenarios, whether the transmitter and receiver are visual line-of-sight (LOS) or non-visual line of sight (NLOS), which usually occurs when one end of the communication link is mobile [8]. In LOS communication, only weather or atmospheric parameters can hinder the communication. The non-line-of-sight (NLOS) communication is quite complicated due to a multitude of various phenomena associated, such as reflections, refraction, diffraction, scattering, and atmospheric absorption [9]. The polarization diversity system, which radiates signals in more than one polarization,

such as horizontal and vertical, can mitigate some of the problems [10].

Slant polarization has built-in polarization diversity as it incorporates both polarizations in itself [11]. It also improves the communication in NLOS scenarios and even in tree foliage [12]. Slant polarization more efficiently caters to the fading problems associated with multipath reflections than horizontal/vertical polarization [13]. Moreover, received signals typically appear at the receiving end more vertically than horizontally polarized due to the physical asymmetries of the vertical and horizontally polarized antenna's construction. Slant-polarization simultaneously generates equal horizontal and vertical components. Hence it can mitigate this problem too [14].

Monopole, dipole [15] antennas are extensively used to produce vertical polarization with omni pattern, while omnidirectional antennas having horizontal polarization usually consist of loop elements [16], [17]. In [18]–[21], the slant-polarized antennas are discussed, which are having directional radiation characteristics instead of omnidirectional characteristics. [19], [22]–[24] Simultaneously produce two linearly polarized waves, which in turn combine to create slant polarized radiation but at the cost of two ports instead of one port with the compulsory ground plane requirement. Thus two-port operation makes these antennas feeding complex and less user friendly. Wherever the metallic surface is available, the antenna operation is not a problem. However, the manufacturing of more lightweight and strong composite materials as compared to metals necessitates that antennas should operate independent of ground plane requirement [25].

For a slant-polarized omnidirectional antenna, it is necessary to have equal horizontal and vertical magnitude components, with 0 phase or 180 phase [26]. Till now there are very few omnidirectional publications which report 45 slant polarization. [25] claims slant polarization with omnidirectional pattern. It is a bifilar helix antenna that actually radiates circular polarization with omnidirectional pattern later verified by [27]. Two dipole elements arranged in orthogonal directions form a basic antenna structure in [28]. Four such elements are printed and wrapped around to form a cylindrical shape. This antenna is energized by the complicated exposed feed network which is placed inside the cylinder. Furthermore, the gain variations in the azimuth pattern are ± 1.0 dB. In [29], there are two topologies which claim to achieve slant polarization omnidirectional radiation. Here an omnidirectional probe having a circular ground plate acts like a monopole. It is further surrounded by eight tilted parallel metal strips which act as parasitic elements in first topology while in second topology; strips are replaced by dielectric strips. Still, they failed to achieve Omni-directionality in azimuth plane and also the feed is not closed. In [30], slot and dipole configurations are used around a cylinder with exposed and complex feed. It reports gain ripple of more than ± 2 dB. In [31], bulky external multi polarizer layers are placed around the vertical polarized biconical antenna. Such

screens resolve the vertical polarization into slant polarization by rotating the polarization plane with a gain ripple of ± 4.8 dB. However, due to the complex and layered structure, it cannot be utilized in all-weather all-season hostile environments. Based on the papers available in the open literature, earlier work on this type of antenna is inadequate.

All of the above antennas have high gain ripple in azimuth plane due to open feed mechanism, which breaks the axis symmetry and reduces radiation efficiency as exposed feed interact with the radiating elements, leading to fluctuation and reduction in coverage range at variant horizontal plane angles.

In this paper, slant polarized omnidirectional antenna, with horizontal gain ripple smaller than ± 0.18 dB, is presented. The proposed antenna consists of rings of slot elements and an internal collinear feed network, which assists in maintaining axis symmetry. The antenna structure is compact, rugged, and (Direct Current) DC grounded. Moreover, the proposed configuration has better polarization purity, as cross-pol are low as compare to that of the co-pol. This is the first time that an antenna is reported which is (Direct Current) DC short, conformal, and having low azimuthal gain variations and aerodynamic drag. The paper flow is such as: in Section 2, antenna configuration is presented; Section 3 consists of feed mechanism; in Section 4, antenna analysis and design topology are discussed; Section 5 describes antenna fabrication and experimental verifications; Section 6 presents a comparison of the proposed work with published work; finally, Section 7 ends with the conclusion.

II. ANTENNA CONFIGURATION

The basic antenna configuration is depicted in Fig. 1. The antenna consists of two basic parts. Radiation parts consist of two oversized cylinders. The medium between the two oversized cylinders is filled with air. The prime radiation source is a slot aperture. A slot is a reciprocal of the dipole radiator having its electric current source replaced by a magnetic one. Slot is etched around the outer most conductor, as shown in Fig. 1(a). The slot is rotated along its axis at an angle. This angled slot will generate a slant wave. Four such slots etched around the outer cylinder form the array and produce slant polarized omnidirectional radiation. The complete antenna is depicted in Fig. 1(a) and (b). The feeding part consists of SMA adaptor of 50-ohm characteristic impedance. The length of the inner SMA conductor is optimized. This length serve as matching which converts standard 50 connector to the oversized inner coaxial conductor, as shown in Fig. 1(b).

The three most critical parameters to produce slant polarization are outer cylinder diameter, slanted slot length and feed pin diameter which connect oversized inner cylinder to outer cylinder. The optimized geometric parameters are summarized in Table.1

For Military operations, antennas should be able to move towards remote, rough, and tough operational area terrains and bear all-weather conditions. Such requirements require the potential antenna must be physically rugged and robust structure and requiring no external spine to support as exterior

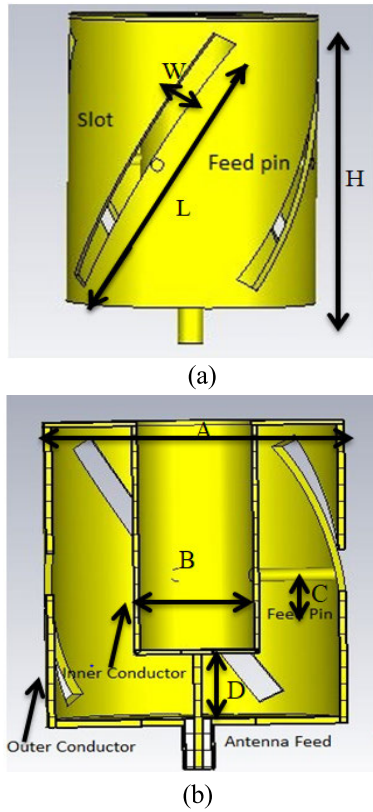


FIGURE 1. Proposed antenna (a) 3D view, (b) cross-sectional view.

TABLE 1. Dimensions of the proposed antenna.

Parameter	Value (mm)	Parameter	Value (mm)
A	60	W	5
B	25	L	65
C	3.0	H	70
D	14.83	α (angle)	32.5°

spines make these antennas bulky [32]. Large antennas also induce more drag, which increases the chances of damages due to turbulent weather conditions and too weak from a structural point of view [16], [32]. So, compact and low wind profile structure should be utilized. Furthermore, Passive Intermodulation PIM can happen in joints which are loosely connected or soldered [33], and also, there is a probability of Peak Instantaneous Power PIP occurring within the feed network, which can quickly damage the PCB based structures [34]. The flaunted antenna, is circumventing these difficulties, as mentioned above. Electrostatic discharge (ESD) and lightning can make their way into the system through the antenna. ESD jeopardizes the reliability and protection of electronic equipment, while lightning can quickly damage the whole system. A DC ground is the most viable and effective

technique applied in military applications [35]. The antenna is mainly made of brass and DC grounded. The whole antenna is axisymmetric.

III. FEED MECHANISM

The antenna shape has to be conformal and like a pole due to aerodynamic and installation space constraint for vehicular or base station applications. In all the references cited above, the feeding mechanism is implemented either on a printed circuit board or through the coaxial cable, which is usually exposed to the antenna elements and not entirely enclosed by the antenna and radiates itself. Thus the feed interferes with the pattern in the azimuth plane and also breaks the axis symmetry. Thus significant gain ripple in the omnidirectional pattern is achieved. Gain ripple deteriorates the required radiation pattern. Moreover exposed feed network makes the antenna too large, which increases the feeding complexity and losses and needs external structures to support.

By making a coaxial feed with all the parts having a common axis, which goes down the center of the radiating element, solves all of the above problems. A significant advantage of this type of feed is that the coaxial structure is closed and does not radiate or interfere with the radiating elements that it feeds. It further reduces the no of elements required to achieve the same gain as compared to antennas with exposed feeding.

The excitation mechanism of the proposed antenna is very simple and straightforward. There are no complex baluns or impedance transformers involved. There are only four feed pins which connect the oversized inner conductor to the angled slots. The optimized height of the inner conductor of the standard SMA guarantees smooth transition of standard Coaxial TEM mode to oversized cable TEM modes, as shown in Fig. 1. The feed and antenna can easily be assembled by sliding the pieces together along the axis.

IV. ANALYSIS AND DESIGN

To successfully design a slant polarized omnidirectional antenna, the required electric fields magnitudes and phase values are as shown in Equation 1 and Equation 2 as explained in [28]:

$$E + 45^\circ = E_\varphi \cos 45^\circ - E_\theta \sin 45^\circ \tag{1}$$

$$E - 45^\circ = E_\varphi \cos 45^\circ + E_\theta \sin 45^\circ \tag{2}$$

E_φ and E_θ are the φ and θ components of the far zone electric field. To produce a true +45° slant polarization, two requirements must be satisfied. The first requirement is that the magnitudes of electric fields oriented along θ and φ directions must be same such as $|E_\theta| = |E_\varphi|$; and the second requirement is the phase difference between orthogonal electric field components should be 180° or $\angle E_\theta - \angle E_\varphi = 180^\circ$. For -45° slant polarization, the first requirement stays the same as dictated by the +45° slant polarization; however, the phase difference, in this case, is 0° or $\angle E_\theta = \angle E_\varphi$.

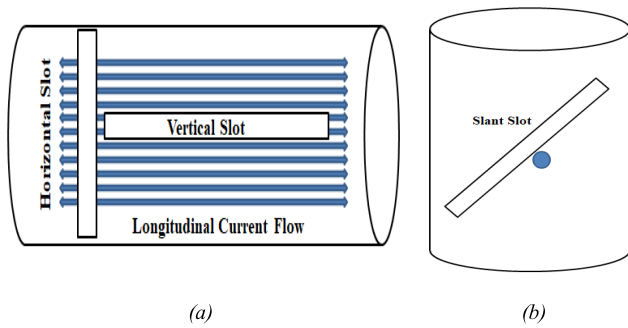


FIGURE 2. Slot Configurations (a) Vertical and horizontal slot (b) Slant slot.

A. BASIC DESIGN

Horizontal slots cut on the outer cylinder of an oversized coaxial constitute vertical polarization because they can easily perturb the longitudinal surface current on the oversized coaxial cable [36], as shown in Fig.2 (a). On the contrary, the longitudinal slots on the outer cylinder cannot be energized due to its parallel orientation with surface current even short-circuiting does not change the surface current orientation [37].

To excite the vertical slots on coaxial, a novel feed mechanism is utilized. Feed pins are placed between the inner and outer conductors of oversized coaxial cable. The slots are excited by only one side, so the opposite side of each slot is floating. The basic building block is a single vertical slot shown in Fig 2(a). The slot is considered as an equivalent dipole [38], so the longitudinal slot is $\lambda/2$ long. Four such slots around the oversized cable axis constitute the primary omnidirectional antenna. As longitudinal slot gives horizontal polarization so by angling the slot around its axis, we can excite both polarizations within the same structure, as shown in Fig 2 (b). By optimizing the slot rotation and the pin feed diameter, balance between the both horizontal and vertical polarization can be achieved. That balance helps to obtain required orthogonal electric fields and their corresponding phase values necessary for ± 45 slant polarization.

B. SIMULATION VERIFICATION

CST Microwave Studio is the software that we have utilized for the simulation and optimization of the slant polarized omnidirectional antenna. Fig. 3 shows the relationship of antenna azimuth gain ripple and no of slots around the antenna axis. The slot produces a directional radiation pattern. As we increase the number of slots around the antenna axis. These directional radiation patterns broaden, which can be seen in Fig. 3. At the optimum value, which in this case, is four slots, these radiation patterns are broad enough so that they overlap and create the slant polarized omnidirectional radiation pattern with very low gain ripple.

C. DETERMINATION OF SLOT ORIENTATION ANGLE

According to the definition of 45° slant polarization, the first necessary condition is to make the ratio of E_θ and E_φ to

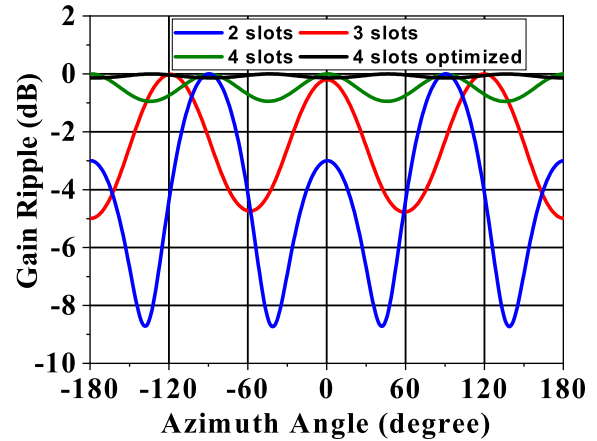


FIGURE 3. Effect on Azimuthal gain ripple by varying the No of Slots around the antenna axis.

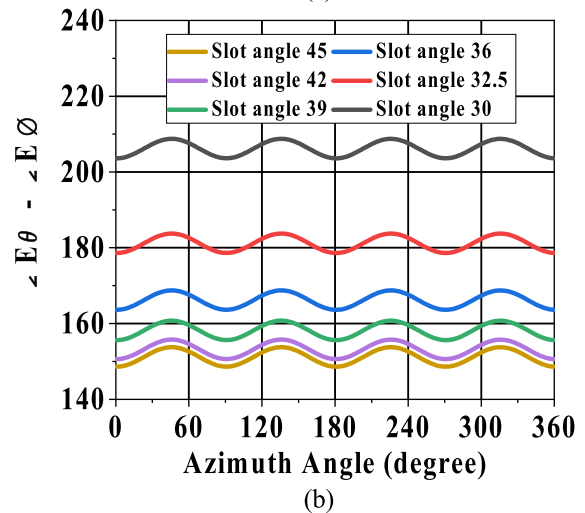
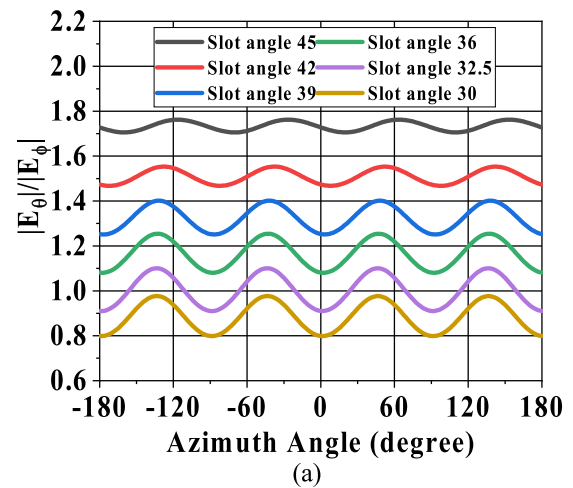


FIGURE 4. (a) Azimuthal magnitude ratio ($|E_\theta|/|E_\varphi|$) (b) Azimuthal phase difference ($\angle E_\theta - \angle E_\varphi$) as a function of orientation angle α .

be unity where the second essential condition requires the phases of E_θ and E_φ equal, i.e., $\angle E_\theta = \angle E_\varphi$, or have a 180° phase difference, i.e., $\angle E_\theta - \angle E_\varphi = 180^\circ$. We calculated the ratio and phases of both E fields with the help of CST by

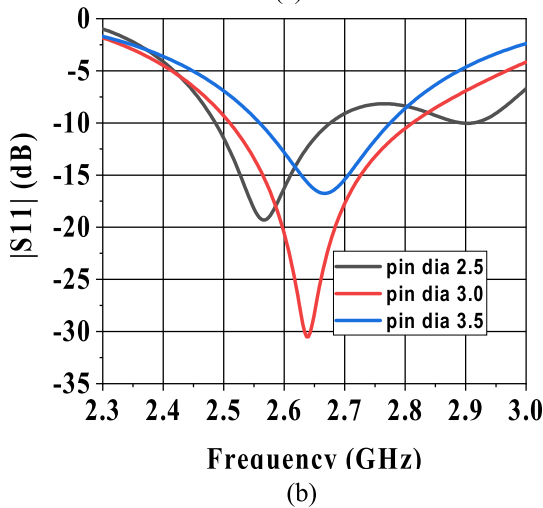
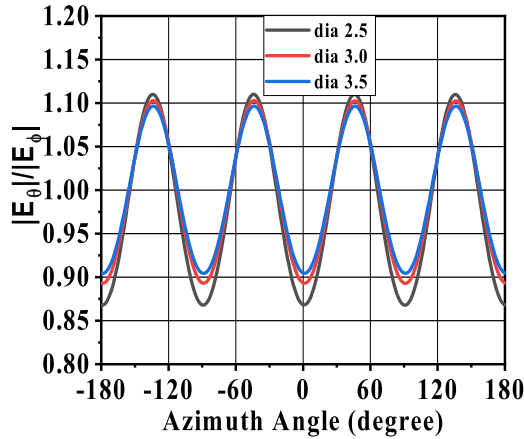


FIGURE 5. (a) Azimuthal magnitude ratio ($|E_{\theta}|/|E_{\phi}|$) (b) Return loss of antenna as a function of feed pin dia.

keeping the slot length constant and plotted as a function of the azimuthal angle for different values of the slot orientation angle α in Fig. 4(a) and (b). It can be seen that when alpha is 45° degree, the ratio varies around 1.8, and peak to peak variations are less than 0.1, and phase variation is 150°. When alpha is 30°, the ratio is less than 0.9, and the variation is 0.2, while that of phase difference is 205°. As alpha is close to 32.5°, the ratio is close to 1, and the peak to peak variation is less than 0.2, and the phase varies around 180. Hence the optimal value for the orientation angle 32.5°.

D. DETERMINATION OF PIN DIAMETER AND SLOT SIZE EFFECT

Fig. 5 shows the effect of the diameter of the pin that is connecting the slant slot to the oversized inner conductor.

The change of diameter does not affect the ratio of E_{θ}/E_{ϕ} , but it changes the matching of the antenna, as shown in Fig. 5(a) and (b). While Fig. 6 (a) shows the effect of the slot length change on the antenna S11, which depicts the length of the slot varies the antenna matching region only. While Fig. 6 (b) portrays optimized ($|E_{\theta}|/|E_{\phi}|$) and phase difference ($\angle E_{\theta} - \angle E_{\phi}$) as a function of frequency for +45° slant

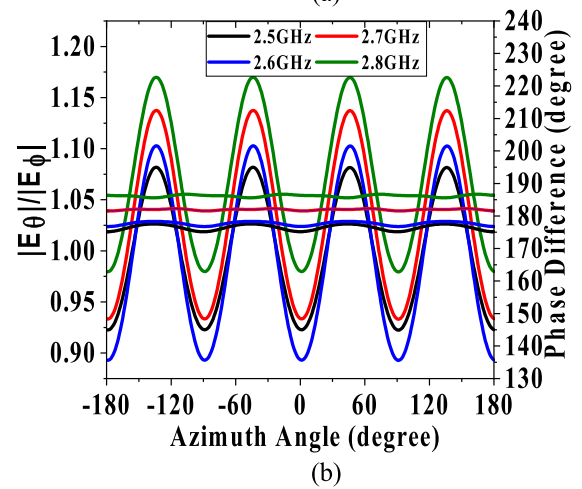
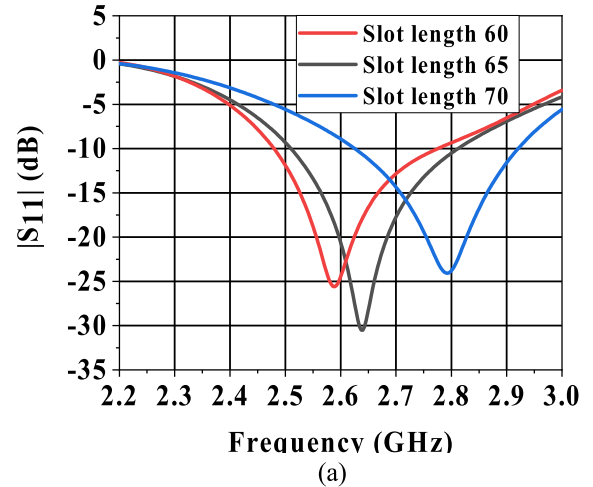


FIGURE 6. (a) Return loss of antenna as a function of slot length (b) Optimized ($|E_{\theta}|/|E_{\phi}|$) and phase difference ($\angle E_{\theta} - \angle E_{\phi}$) as a function of frequency.

polarization. The optimized slot rotation angle α is 32.5°, with feed pin diameter is 3 mm. The ratio of $|E_{\theta}|/|E_{\phi}|$ is fluctuating around 1 with a variation value of ± 0.15 . The phase value is $\angle E_{\theta} - \angle E_{\phi} = 180 \pm 5^\circ$ throughout the frequency range (2.5GHz to 2.8 GHz). To realize opposite polarization such as -45° slant polarization, only reverse the slot orientation and the pin feed location.

E. FIELD VERIFICATION

The cross-sectional view of electric fields at the feed point and at the slot pin feed position are shown in Fig. 7(a) and (b), while that of the H-fields are depicted in Fig. 7(c) and (d). At the feed point of the antenna, E filed is radially outward distributed (TEM mode). While at the start of the oversized inner cylinder, the E filed is again radially outward as that of TEM mode. This shows that the optimized height of the inner conductor of the SMA connector has successfully transformed the connector TEM mode to the oversized coaxial assembly TEM mode. As it moves towards the feed pin, the field starts to circulate the slot. All the slot fields have the same circulation patterns, which show they add in phase,

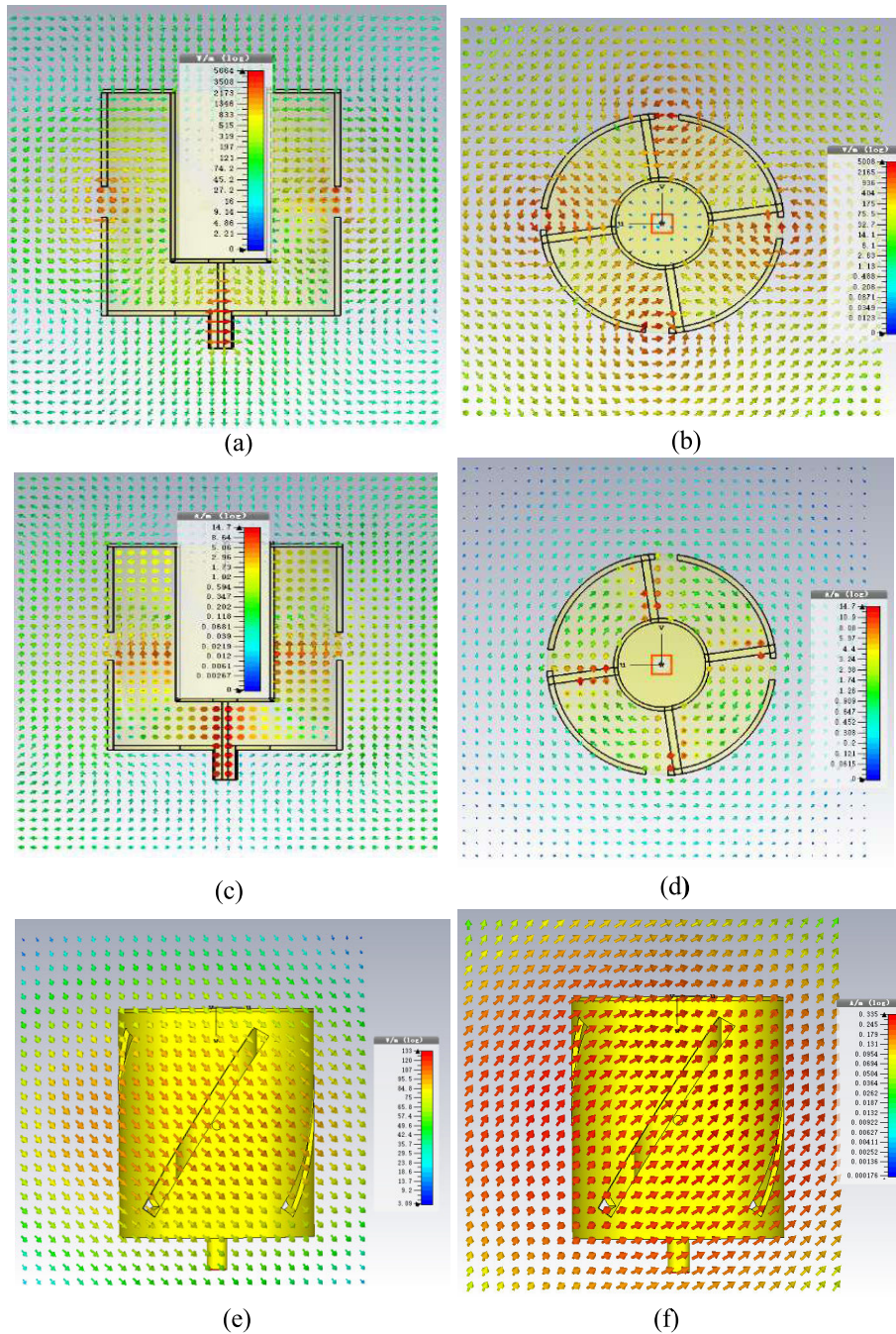


FIGURE 7. (a) The cross-sectional view of electric fields along YZ plane (b) The cross-sectional view of electric fields along XY plane at slot pin feed (c) The cross-sectional view of magnetic fields along YZ plane (d) The cross-sectional view of magnetic fields along XY plane at slot pin feed (e) The view of electric fields outside of antenna along YZ plane (f) The view of magnetic fields outside of antenna along YZ.

as shown in Fig. 7(b). The electric field progressively moves away from the slot center to the ends and thus radiates a slant polarized field. The directional slot radiation patterns are broad enough so that they overlap and create the omnidirectional, slant polarized outward traveling wave. Similarly, the H field forms a closed-loop (TEM mode) at the input Fig. 7 (c) while outside the antenna H field perpendicular to the corresponding E field, as shown in simulated field

distributions in Fig. 7 (d). Fig. 7(e) and (f) show the electric and magnetic fields radiated outside the antenna structure which clearly shows slant polarized outward waves

V. ANTENNA FABRICATION AND MEASUREMENT RESULT

To validate the concept, an antenna is manufactured. Measured and simulated results of the proposed antenna are presented in this section. Fig. 8 shows a picture of the antenna



FIGURE 8. Fabricated prototype antenna.

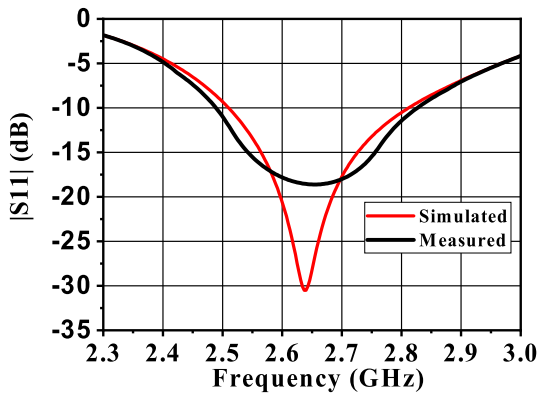


FIGURE 9. Simulated and measured S-parameters antenna.

prototype. The return loss of the fabricated prototype was performed on an Agilent VNA. In Fig. 9, the reflection coefficient obtained by measurement and simulation is plotted. They are less than -10 dB from 2.5 GHz to 2.8 GHz.

These results are in good agreement with simulation but shifted to the lower frequency because of manufacturing errors. This antenna can be manufactured through CNC machine or by costly direct metal printing such as the additive 3D metal printing. The antenna is having very small foot print and also conformal so it will sustain very low wind loading. Considering the size, the antenna is a quite wideband structure (11.3 % bandwidth). Measured and simulated radiation patterns of the antenna are shown in Fig. 10. Radiation patterns are plotted at 2.5 GHz and 2.8 GHz, respectively. Patterns were recorded along vertical elevation plane and horizontal azimuth planes of the antenna, respectively. Fig. 10(a)–(d) shows the simulated and measured Co-pol (normalized) and simulated Cross-pol radiation pattern (normalized) in the omnidirectional plane (H-plane) and elevation-plane (E-plane). The cross-pol levels in the azimuth plane are more than 14dB lower than the desired polarization. Simulations and measurements are well matched. The 360° or omnidirectional radiation at the horizontal plane

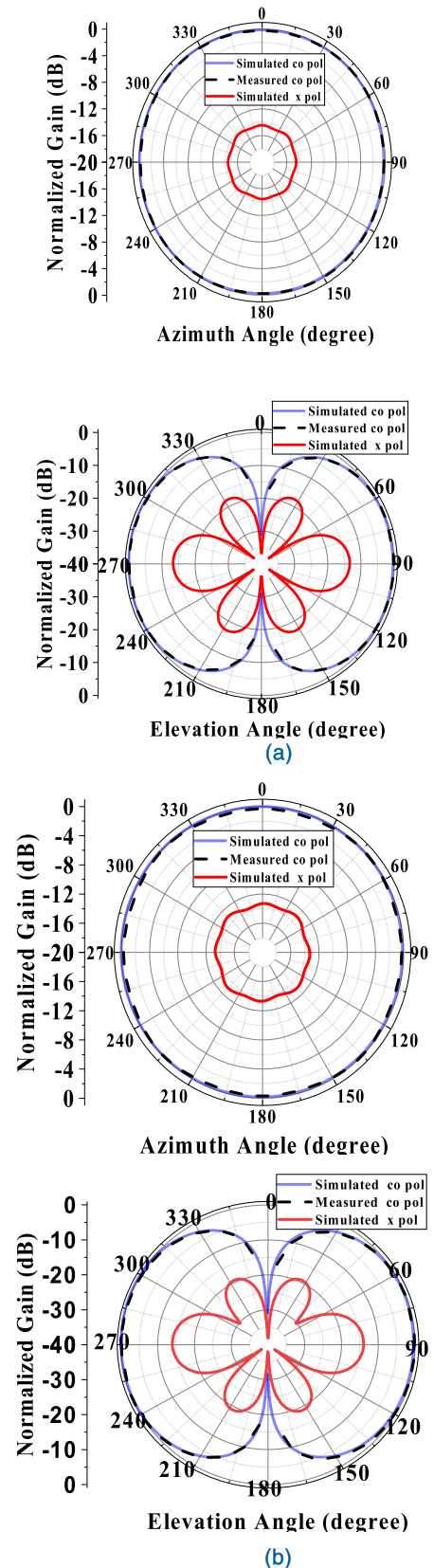


FIGURE 10. Simulated normalized Co and Cross pol radiation patterns and measured normalized radiation pattern in the omnidirectional plane or H-plane on the top row while E-plane on the bottom row (a) 2.5 GHz. (b) 2.8 GHz.

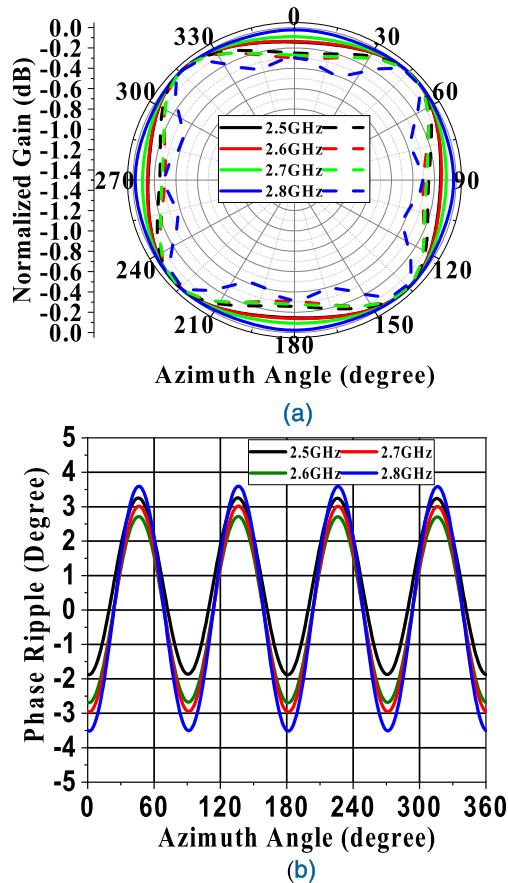


FIGURE 11. (a) Measured normalized Gain Ripple in the omnidirectional plane or H plane (solid lines simulated, dashed lines measured) (b) measured normalized Phase Ripple in the omnidirectional plane or H plane as a function of frequency.

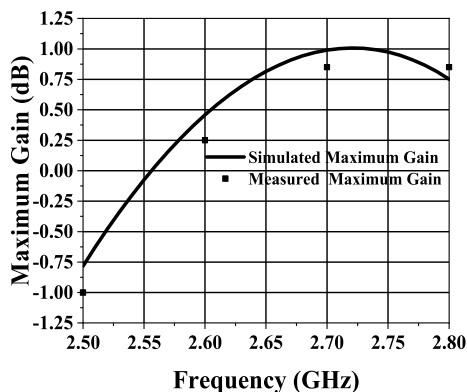


FIGURE 12. Simulated and measured antenna gain.

guarantees all yaw angle operability. Moreover, this omnidirectional feature of the antenna remains steady from lower bounds to the upper limits of the operational bandwidth, as shown in Fig. 10. In Fig. 11(a) the measured normalized azimuth gain ripple is shown in polar plot for clear visibility of the gain ripple values. The maximum peak to peak value is 0.4 dB or ± 0.2 dB in the azimuth plane confirming a good omnidirectionality. Fig. 11(b) shows the azimuth pattern phase ripple which is having only 7° phase ripple peak to

TABLE 2. Comparison of proposed work with previous work.

Ref	Pattern Type	Dimension (HxWxL) λ^3	Gain Ripple (dB)	DC Ground	Feed Type
[30]	Omni	0.51x0.51x0.67	± 1.0	No	Exposed
[31]	Not-Omni at horizon	0.93x0.93x0.61	NA	No	Exposed
[32]	Omni	0.38x0.38x0.67	± 2.0	No	Exposed
[33]	Omni	0.80x0.80x0.56	± 4.8	No	Exposed
Proposed work	Omni	0.53x0.53x0.61	± 0.2	Yes	Enclosed

peak. Both figures confirm the excellent pattern stability versus frequency of the proposed antenna. Fig. 12 illustrates simulated and measured gain of the flauented antenna throughout the operating frequency range. This DC ground and rugged antenna achieve stable gain within the whole band. These results demonstrate very encouragingly, and useful radiation features at yaw angles, paving the way to make this antenna a right choice for direction-finding and mobile communication applications.

VI. COMPARISON

A comparison of the proposed work with previously published works having slant polarization is shown in Table 2. There are only four publications which are slant polarized and also omnidirectional. The proposed antenna is novel because it has an internal axis-symmetric feed network. All other omnidirectional antennas compared in the table are designed with exposed feed. Furthermore, this antenna first time achieves the slant polarization with the help of slot radiators and gives stable azimuthal gain at the horizon angle as compared to other omnidirectional designs. Moreover, it is DC ground, with low gain ripples.

VII. CONCLUSION

A new slant polarized omnidirectional antenna based on the slot configuration with novel feed arrangement is presented. By mounting four-slots around the antenna axis and exciting them with a compact internal feed network, stable gain with enhanced polarization purity is achieved in azimuth plane throughout the operational band. As the internal axis-symmetric closed feed structure does not radiate or interfere with the radiating elements, a low azimuth gain ripple is achieved. Stable gain in azimuth (yaw) plane with low ripples is favorable in direction finding and communication applications. The antenna can be scalable to control the gain requirements accordingly. Other than scalability and electromagnetic characteristics, it also has the required mechanical properties that are necessary for its smooth operation in the rough environment. This antenna possesses a physically tough, DC grounded, rugged structure and requiring no external spine to support itself. Conformal and Compact shape

induces less drag and reduces chances of damage due to all weather and terrain conditions for military missions. Furthermore, the low gain ripple in the omnidirectional pattern may reduce the fluctuation in the coverage area or increase link efficiency.

REFERENCES

- [1] H. Nawaz, X. Liang, M. S. Sadiq, J. Geng, W. Zhu, and R. Jin, "Ruggedized planar monopole antenna with a null-filled shaped beam," *IEEE Antennas Wireless Propag. Lett.*, vol. 17, no. 5, pp. 933–936, May 2018.
- [2] H. Nawaz, X. Liang, M. S. Sadiq, J. Geng, and R. Jin, "Circularly-polarized shaped pattern planar antenna for aerial platforms," *IEEE Access*, vol. 8, pp. 7466–7472, 2020.
- [3] M. Wasif Niaz, M. Shahzad Sadiq, Y. Yin, S. Zheng, and J. Chen, "Reduced aperture low sidelobe patch array," *Electron. Lett.*, vol. 54, no. 13, pp. 800–802, Jun. 2018.
- [4] M. A. Salari, O. Manoochehri, A. Darvazehban, and D. Erricolo, "An active 20-MHz to 2.5-GHz UWB receiver antenna system using a TEM horn," *IEEE Antennas Wireless Propag. Lett.*, vol. 16, pp. 2432–2435, 2017.
- [5] A. Darvazehban, O. Manoochehri, M. A. Salari, P. Dehkhoda, and A. Tavakoli, "Ultra-wideband scanning antenna array with rotman lens," *IEEE Trans. Microw. Theory Techn.*, vol. 65, no. 9, pp. 3435–3442, Sep. 2017.
- [6] O. Manoochehri, A. Darvazehban, M. Salari, S. Khaledian, D. Erricolo, and B. Smida, "Dual-polarized biconical antenna for direction finding applications from 2 to 18 GHz," *Microw. Opt. Technol. Lett.*, vol. 60, pp. 1552–1558, May 2018.
- [7] Y. C. Moon, O. S. Choi, I. H. Kim, and H. S. Yang, "Omnidirectional antenna for mobile communication service," U.S. Patent 0170550 A1, Jun. 15 2017.
- [8] M. Ding, P. Wang, D. Lopez-Perez, G. Mao, and Z. Lin, "Performance impact of LoS and NLoS transmissions in dense cellular networks," *IEEE Trans. Wireless Commun.*, vol. 15, no. 3, pp. 2365–2380, Mar. 2016.
- [9] T. S. Rappaport, *Wireless Communications: Principles and Practice*, 2nd ed. Upper Saddle River, NJ, USA: Prentice-Hall, 2001, pp. 78–80.
- [10] B. Lindmark and M. Nilsson, "On the available diversity gain from different dual-polarized antennas," *IEEE J. Sel. Areas Commun.*, vol. 19, no. 2, pp. 287–294, 2001.
- [11] J. J. A. Lempiainen and J. K. Laiho-Steffens, "The performance of polarization diversity schemes at a base station in small/micro cells at 1800 MHz," *IEEE Trans. Veh. Technol.*, vol. 47, no. 3, pp. 1087–1092, Aug. 1998.
- [12] T.-C. Tu, C.-M. Li, and C.-C. Chiu, "The performance of polarization diversity schemes in outdoor micro cells," *Prog. Electromagn. Res.*, vol. 55, pp. 175–188, 2005.
- [13] U. Wahlberg, "Polarization diversity for cellular base stations at 1800 MHz," Allgon System AB, Kista, Sweden, Tech. Rep. T1017, Jan. 1997.
- [14] B. Lindmark, "A Beamwidth Definition for Slanted Dual-polarized Base Station Antennas," *Microw. J.*, vol. 40, no. 5, May 1997, pp. 324–328.
- [15] C. A. Balanis, *Antenna Theory Analysis and Design*, 3rd ed. Tempe, AZ, USA: Wiley, 2005, pp. 170–184.
- [16] X. L. Quan, R. Li, J. Y. Wang, and Y. H. Cui, "Development of a broadband horizontally polarized omnidirectional planar antenna and its array for base stations," *Prog. Electromagn. Res.*, vol. 128, pp. 441–456, 2012.
- [17] K. Wei, Z. Zhang, Z. Feng, and M. F. Iskander, "A MNG-TL loop antenna array with horizontally polarized omnidirectional patterns," *IEEE Trans. Antennas Propag.*, vol. 60, no. 6, pp. 2702–2710, Jun. 2012.
- [18] M. Hajj, R. Chantalat, T. Monediere, and B. Jecko, "A 45° linearly polarized sectoral antenna with M-EBG structure for WiMAX base stations," *IEEE Antennas Wireless Propag. Lett.*, vol. 9, pp. 737–740, 2010.
- [19] K. Gosalia and G. Lazzi, "Reduced size, dual-polarized microstrip patch antenna for wireless communications," *IEEE Trans. Antennas Propag.*, vol. 51, no. 9, pp. 2182–2186, Sep. 2003.
- [20] Q. Zhang and Y. Lu, "45° linearly polarized substrate integrated waveguide-fed slot array antennas," in *Proc. Int. Conf. Microw. Millim. Wave Technol.*, Apr. 2008, pp. 1214–1217.
- [21] V. F. Fusco and P. Hanumantha Rao, "Wide-band dual slant linearly polarized antenna," *IEEE Trans. Antennas Propag.*, vol. 51, no. 8, pp. 2014–2019, Aug. 2003.
- [22] H. Nakano, N. Suzuki, T. Ishii, and J. Yamauchi, "Mesh antennas for dual polarization," *IEEE Trans. Antennas Propag.*, vol. 49, no. 5, pp. 715–723, May 2001.
- [23] R. R. Ramirez and F. D. Flaviis, "Dual band dual linear polarization elliptical microstrip ring antenna," in *Proc. Int. Symp. Antennas Propag.*, Jul. 1999, vol. 3, pp. 1636–1639.
- [24] A. Ando, N. Kita, W. Yamada, K. Itokawa, and A. Sato, "Study of dual-polarized omni-directional antennas for 5.2 GHz-band 2/spl times/2 MIMO-OFDM systems," in *Proc. IEEE Antennas Propag. Soc. Symp.*, Dec. 2004, pp. 1740–1743.
- [25] M. Amin, R. Cahill, and V. Fusco, "Single feed low profile omnidirectional antenna with slant 45° linear polarization," *IEEE Trans. Antennas Propag.*, vol. 55, no. 11, pp. 3087–3090, Nov. 2007.
- [26] M. S. Sadiq and C. Ruan, "A compact, mechanically rugged, DC grounded 45° slant polarized low gain ripple omnidirectional antenna," in *IEEE MTT-S Int. Microw. Symp. Dig.*, Guangzhou, China, May 2019, pp. 1–3.
- [27] S. Iqbal, M. Amin, and J. Yousaf, "Low profile circularly polarized side-fed bifilar helix antenna," in *Proc. 9th Int. Bhurban Conf. Appl. Sci. Technol. (IBCAST)*, Jan. 2012, pp. 325–328.
- [28] X. Quan, R. Li, Y. Fan, and D. E. Anagnostou, "Analysis and design of a 45° slant-polarized omnidirectional antenna," *IEEE Trans. Antennas Propag.*, vol. 62, no. 1, pp. 86–93, Jan. 2014.
- [29] Y. M. Pan, S. Y. Zheng, and B. J. Hu, "Singly-Fed Wideband 45° Slant-Polarized Omnidirectional Antennas," *IEEE Antennas Wireless Propag. Lett.*, vol. 13, pp. 1445–1448, 2014.
- [30] H. Arai, B. Rohani, and R. Kaneda, "Slant 45° polarized multi-frequency cylindrical slot-dipole antenna," in *Proc. 6th Asia-Pacific Conf. Antennas Propag. (APCAP)*, Xi'an, China, Oct. 2017, pp. 1–3.
- [31] A. Dastranj and B. Abbasi-Arand, "High-performance 45° slant-polarized omnidirectional antenna for 2–66-GHz UWB applications," *IEEE Trans. Antennas Propag.*, vol. 64, no. 2, pp. 815–820, Feb. 2016.
- [32] Y. Cui, P. Luo, Q. Gong, and R. Li, "A compact tri-band horizontally polarized omnidirectional antenna for UAV applications," *IEEE Antennas Wireless Propag. Lett.*, vol. 18, no. 4, pp. 601–605, Apr. 2019.
- [33] Commscope. *PIM Happens*. Accessed: Nov. 1, 2020. [Online]. Available: www.commscope.com
- [34] R. Daly, "Development of omnidirectional collinear arrays with beam stability for base station and mobile applications," M.S. thesis, Elect. Comput. Eng., RMIT Univ., Melbourne, VIC, Australia, 2015.
- [35] K. Fujita, "MNL-FDTD/SPICE method for fast analysis of short-gap ESD in complex systems," *IEEE Trans. Electromagn. Compat.*, vol. 58, no. 3, pp. 709–720, Jun. 2016.
- [36] K. Iigusa and M. Tanaka, "A horizontally polarized slot-array antenna on a coaxial cylinder," in *Proc. Asia-Pacific Microw. Conference. Process.*, Sydney, NSW, Australia, 2000, pp. 1444–1447.
- [37] H. Ohmine, Y. Sunahara, S. Sato, T. Katagi, and S. Wadaka, "Omnidirectional slot antenna," U.S. Patent 5 717 410, Feb. 10, 1998.
- [38] B. Zhou, J. Geng, X. Bai, L. Duan, X. Liang, and R. Jin, "An omnidirectional circularly polarized slot array antenna with high gain in a wide bandwidth," *IEEE Antennas Wireless Propag. Lett.*, vol. 14, pp. 666–669, 2015.



MUHAMMAD SHAHZAD SADIQ (Graduate Student Member, IEEE) was born in Karachi, Pakistan, in 1983. He received the B.E. degree in electrical engineering from the University of Engineering and Technology Lahore, Pakistan, in 2005, and the M.S. degree in electrical engineering from the Nanjing University of Aeronautics and Astronautics, Nanjing, China, in March 2012. He joined Margalla Electronics, in 2007, where he is currently a Manager with the Antenna Division. He is responsible for the design, development and qualified testing of antennas for various airborne and ground based communication systems. He joined the School of Electronics and Information Engineering, Beihang University, Beijing, China, as a Ph.D. Scholar, in September 2018. His current research interests include airborne antennas and high-gain omnidirectional antennas.



CUNJUN RUAN (Senior Member, IEEE) was born in Gansu, China, in 1974. He received the M.Ph. and Ph.D. degrees in physics from Tsinghua University, Beijing, China, in 2003. Since 2003, he has been with the Institute of Electronics, Chinese Academy of Sciences, Beijing, where he is involved in sheet beam klystron (SBK), extended interaction klystron (EIK), and integrated vacuum electronics (IVE). He was an Assistant Professor, an Associate Professor, and a Professor, in 2003, 2006, and 2011, respectively. Since 2014, he has been with the School of Electronics and Information Engineering, Beihang University, Beijing. He focuses his research on the interaction processes and physical analysis between terahertz wave and related materials, spectroscopy, and imaging in the security field. His current research interests include high-power and broadband radiation sources in millimeter-wave and terahertz band, such as SBK, EIK, and TWT, and integrated semiconductor vacuum tube with high power, continuous-wave, and broadband in the terahertz range.



HAMZA NAWAZ received the B.S. degree in electrical (telecommunication) engineering from the COMSATS Institute of Information Technology, Islamabad, Pakistan, in 2011. He is currently pursuing the M.S. degree in electronics science and technology (focused on electromagnetics) with the Modern Antenna Research Center, Shanghai Jiao Tong University, Shanghai, China.

From 2011 to 2012, he worked as a RF Design Engineer. From 2012 to 2017, he was an Assistant Manager Telecommunication with Advanced Engineering Research Organization, Pakistan. He has authored or coauthored 20 publications in peer-reviewed international journals and conferences. His research interests include RF and microwave circuits, dielectric resonator antennas, beam-shaped antennas, and partial reflecting surfaces.



SHAHID ULLAH was born in Bannu, Pakistan, in 1990. He received the B.S. degree in telecommunication from the University of Science and Technology Bannu, Pakistan, in 2013, and the M.S. degree in electrical engineering from the Comsat Institute of Information Technology, Islamabad, Abbottabad, Pakistan, in July 2016. He joined the B.Tech. (Telecom.) Department, Bannu University of Science and Technology, as a Visiting Lecturer, in September 2016. He did his research work on Multiband rectenna design. He joined the School of Electronics and Information Engineering, Beihang University, Beijing, China, as a Ph.D. Scholar, in September 2017. His current research interests include metamaterial, antenna design, and terahertz technology.

WENLONG HE (Member, IEEE) received the Ph.D. degree in relativistic electron beams and masers from the University of Strathclyde, Glasgow, U.K., in 1995. He was a Senior Research Fellow with the Scottish Universities Physics Alliance, Department of Physics, University of Strathclyde. Since November 2018, he has been the Chair Professor with the College of Electronics and Information Engineering, Shenzhen University, China. His main research interests include relativistic electron beams, gyrotron traveling-wave amplifier (gyro-TWA)/backward-wave oscillators, cyclotron auto-resonance masers (CARMs), free-electron lasers (FELs), and other high-power microwave and terahertz devices.

• • •